Nuclear Materials and Energy 9 (2016) 539–546

Contents lists available at ScienceDirect

Nuclear Materials and Energy

journal homepage: www.elsevier.com/locate/nme

Evaluation of helium effect on ion-irradiation hardening in pure tungsten by nano-indentation method

Zhexian Zhang[a,b,*], Eva Hasenhuetl[a], Kiyohiro Yabuuchi[b], Akihiko Kimura[b]

[a] Graduate School of Energy Science, Kyoto University, Yoshida-honmachi, Sakyo-ku, Kyoto 606-8501, Japan
[b] Institute of Advanced Energy, Kyoto University, Gokasho, Uji, Kyoto 611-0011, Japan

ARTICLE INFO

Article history:
Received 25 November 2015
Revised 7 June 2016
Accepted 14 June 2016
Available online 24 June 2016

Keywords:
Tungsten (W)
Nano-indentation
Size effect
Helium effect
Irradiation hardening

ABSTRACT

As-received and recrystallized pure tungsten (W) were irradiated with 6.4 MeV Fe^{3+} up to 2 dpa with or without He^{+} at 300 °C, 500 °C, 700 °C and 1000 °C respectively. Irradiation hardening was measured by the nano-indentation method. An equation to evaluate the bulk equivalent hardness was derived on the assumption that the geometrically necessary dislocation (GND) densities at an indentation depth were the same before and after irradiation. Ion-irradiation always induces hardening in both as-received and recrystallized W at all the experiment temperatures. In the case of single-beam irradiation, the recrystallized W exhibited higher hardening than as-received one. The effect of helium on the irradiation hardening is dependent on the material condition: as-received W showed an additional hardening by helium at all the irradiation temperatures, while in recrystallized W the hardening was not affected by helium below 700 °C.

1. Introduction

Tungsten was selected as the armor material for ITER diverter and has been considered as a candidate first-wall material for DEMO-like reactors. Since the armor and first wall will receive both high neutron irradiation and high heat flux, researches on irradiation effects on W at a wide variety of temperatures have been conducted so far: microstructure evolution under self-ion irradiation [1–3], alien heavy ion irradiation [2,4,5] and helium [6–8] or deuterium-ion implantations [9]. Special attention was paid to the recrystallization effects on the formation of irradiation-induced microstructures as recrystallization may occur in the materials after suffering high heat load during operation. As for neutron irradiation effect, Fukuda et al. reported irradiation hardening up to 0.47 dpa was highest at 583 °C in the irradiation temperature range from 531 °C to 756 °C [10]. They also reported that recrystallized W showed a larger hardening than the stress relieved (as-received) W after neutron irradiation at 600 °C and 800 °C [11]. However, irradiation data of W is still insufficient especially combined with detailed characterization of the irradiation-induced microstructures which are strongly correlated to the mechanical properties.

In the previous studies on ion-irradiation effects in W [4,12–14], nano-indentation method was adopted to measure the ion-irradiation hardening because of the limitation of the damaged depth to less than several microns. Himei et al. reported that helium in the dual-beam irradiation will enhance the growth of dislocation loops and cavities and therefore increase hardening [4]. Because the ion-irradiated material has a depth dependent profile of displacement damages, the radiation damage microstructures are heterogeneously distributed, which should be taken into account when evaluating ion-irradiation hardening by means of nano-indentation method.

Although the nano-indentation method is effective to measure the ion-irradiation hardening, there is a technical issue of size effect [15] introduced by Nix-Gao model. The size effect is sometimes described by “the smaller, the harder”, which means when indented in a shallow depth, the hardness will be larger than in deeper depth.

The equation derived from the Nix-Gao model is written as:

$$\left(\frac{H}{H_0}\right)^2 = 1 + \frac{h^*}{h} \tag{1}$$

Where H_0 stands for the original hardness of the material or “bulk equivalent hardness”. H is the hardness measured at a depth

* Corresponding Author: Fax: +81 774 38 3479.
E-mail addresses: zx-zhang@iae.kyoto-u.ac.jp (Z.X. Zhang), eva-hasenhuetl@iae.kyoto-u.ac.jp (E. Hasenhuetl), k-yabuuchi@iae.kyoto-u.ac.jp (K. Yabuuchi), kimura@iae.kyoto-u.ac.jp (A. Kimura).

http://dx.doi.org/10.1016/j.nme.2016.06.010

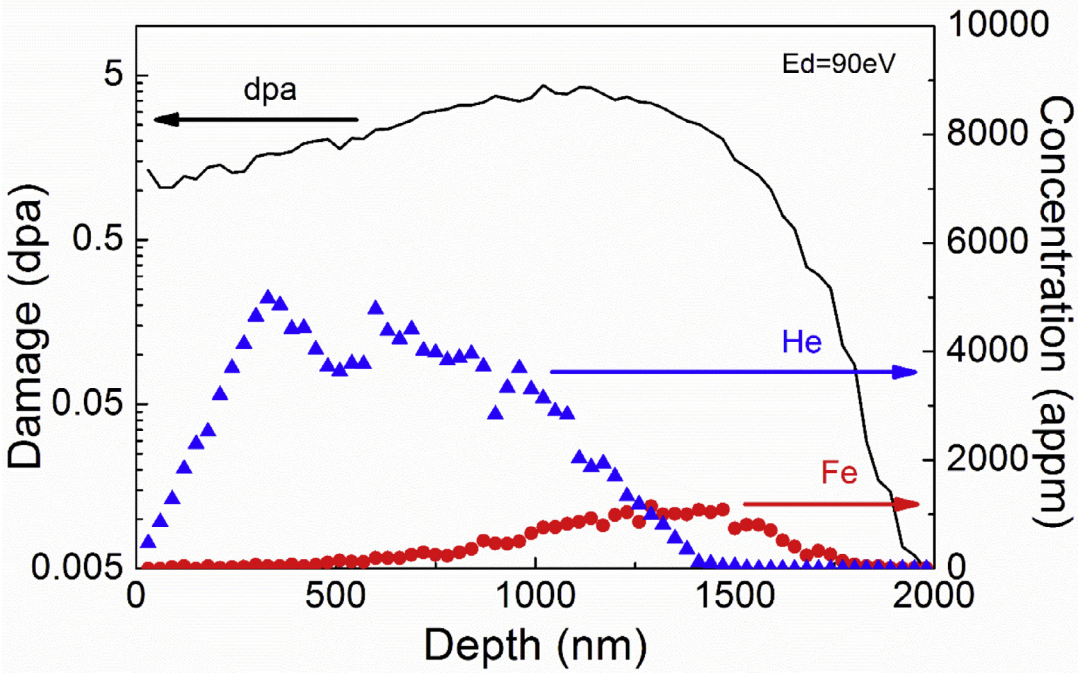

Fig. 1. Depth profiles of damage, He concentration and Fe concentration calculated by SRIM.

Table 1
Chemical composition of as-received tungsten sheet (μg/g).

W	Mo	Fe	Cr	C	Ta	P	O	Si	N	S	Nb	Al
matrix	<100	<30	<20	<30	<20	<20	<20	<20	<5	<5	<10	<15

h, and h^* is a characteristic length. Kasada et al. applied this model to evaluate ion-irradiation hardening, where H_0 was the intercept given by the linear relation between inverse depth (h^{-1}) and hardness (H) in the irradiated area [16,17]. However, in tungsten, the Nix-Gao plots never draw a straight line, even before ion-irradiation. The shortcomings from the application of Nix-Gao model were discussed by Pharr et al.[18], one speculation of which is in the shallow area the model would overestimate the density of GNDs. Huang et al. [19] modified the model with the assumption that there is a saturation of GND density in the shallow area. An EBSD observation suggested the GNDs might transform into subgrain boundaries.As a result, the size effect will be induced by not only GNDs but also multiplication of grain boundaries [20]. The TEM observation of the cross-section of indented region by Katoh et al. [21] revealed that in ferrous alloys the GND affected zone strongly depended on the indentation depth: the GND zone was anisotropic when the indentation depth is less than 100 nm, but it was quite semispherical when exceeding 300 nm. These phenomena indicate that Nix-Gao model does not fit at a shallow area but fits well in deep area. As a result, the bulk-equivalent hardness of the unirradiated specimen could still be estimated by Nix-Gao plots of the deeper area. The hardness of the irradiated layer in the shallow area needs a more adequate evaluation method.

In this research, we investigated the effect of helium on the ion-irradiation hardening of W with and without recrystallization at a wide range of irradiation temperatures by means of nano-indentation method.

2. Experimental procedure

The material used in this research was commercial 99.95 wt% pure rolled W from Nilaco Co. Ltd, denoted as “as-received”, with an average grain size of 1.7 μm. The impurity concentrations are listed in Table 1. Recrystallized W was obtained from as-received one annealed at 1400 °C for 1 h, with an average grain size of 27 μm. The specimens for ion-irradiation experiments were mechanically polished with SiC emery papers of #500~4000 and buff-polished with diamond pastes until a powder diameter of 0.25 μm. Finally the surface was electrolytically polished with a 1% NaOH aqueous solution at a constant voltage of 20 V at ambient temperature.

Ion-irradiations were performed using a dual ion-beam accelerator in Kyoto University, DuET, which could yield a beam of 6.4 MeV Fe^{3+} ions and an energy-degraded beam from 1 MeV He^+ ions simultaneously. For dual ion-beam irradiation, an energy degrader was set up to get a rather homogeneous injection of He^+ which resulted in a total He concentration of 3000 appm in the range of 1.5 μm depth. The irradiation temperatures were 300 °C, 500 °C, 700 °C and 1000 °C. Fig. 1 shows the depth profile of damage and the concentration of implanted elements, which were simulated by SRIM software [22] and calculated following the “Energy damage” method introduced by Stoller et al. [23]. The threshold energy was selected as 90 eV [24]. The averaged dpa of the 2 μm irradiation area is about 2 dpa.

Nano-indentation hardness was measured by Agilent Technologies Inc. Model Nano Indenter G200 with a Berkovich tip. CSM method was applied with the area function calibrated on standard fused silica by Oliver and Pharr method [25]. The nominal strain rate was 0.05 /s and the oscillations set as 2 nm. The maximum penetrating depth was 2000 nm. Testing temperature was controlled to 25 ± 4°C. For an ideal Berkovich tip, the area-function, A, is defined as $A = 24.56\,h^2$, where h is indentation depth. Since nano-indentation hardness is remarkably affected by A, the tip blunting that alters h, should be considered. The area-function

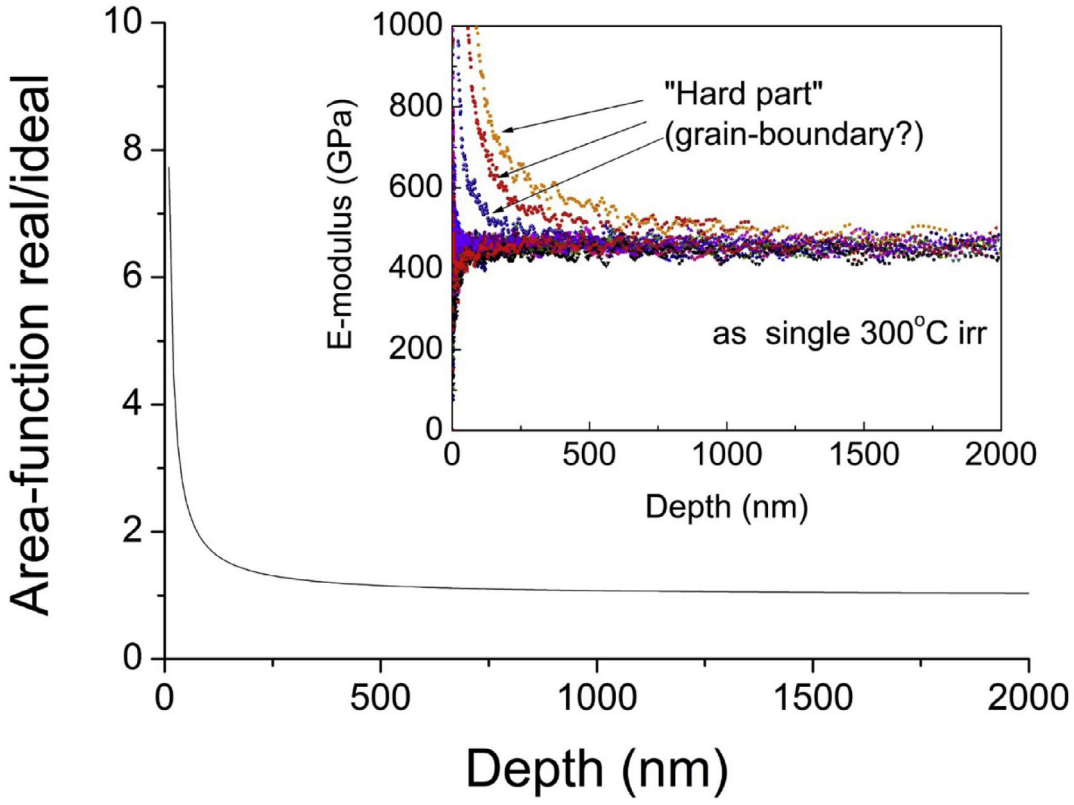

Fig. 2. The ratio of real/ideal area-function, versus indentation depth with an example of elastic modulus obtained by using the area-function.

ratio between the practical tip and an ideal one is shown in Fig. 2. Besides, an example of E-modulus estimated using the area-function is shown in order to indicate that the test condition and parameters we used are adequate.

Microstructures were observed by a JEOL JEM-2010 transmission electron microscope (TEM) at 200 keV. The specimens were produced by focused ion beam (FIB) system (HITACHI FB2200). To remove the damaged region by FIB, the specimens were electrolytically polished in a 0.45% NaOH aqueous solution at 3 °C.

3. Analysis of Nano-indentation hardness

There have been at least two analytical methods applied to evaluate the ion-irradiation hardening by nano-indentation method. One is that the hardness before irradiation, $H_{tested,unirr}$, is directly subtracted from the hardness after irradiation, $H_{tested,irr}$, (see Eq. (2)), based on the assumption that the size effect is the same for the hardness before and after irradiation, although this assumption is not based on theoretical model.

$$\Delta H = H_{tested,irr} - H_{tested,unirr} \tag{2}$$

Another method is an application of Nix-Gao model which provides the bulk-equivalent hardness H_0 in the Eq. (1), based on the assumption that an indentation results in the generation of GNDs within the semi-sphere under the indent. The GND theory has been widely accepted and frequently used currently.

Voyiadjis and Peters [26] elaborated the gradient plasticity theory. Assuming the shear stress, τ, of the material is determined by both of the contributions of statistically stored dislocations (SSD) and GND, can be shown by Eq. (5), where ρ_S and ρ_G are the density of SSD and GND, respectively, μ is the shear modulus, b is the burgers vector, and α is the hardening factor.

$$\tau_G = \alpha\mu b\sqrt{\rho_G} \tag{3}$$

$$\tau_S = \alpha\mu b\sqrt{\rho_S} \tag{4}$$

$$\tau = \left(\tau_S^2 + \tau_G^2\right)^{1/2} \tag{5}$$

The relationship between hardness H, tensile stress σ and shear stress τ, can be written as:

$$\sigma = M\tau \tag{6}$$

$$H = k\sigma \tag{7}$$

where M stands for Taylor's factor, k is the coefficient between hardness and tensile stress. SSD can be taken as the contributor of the intrinsic hardness. Therefore, the bulk-hardness, H_0, which can be interpreted in terms of intrinsic hardness without size effect, is written as:

$$H_0 = kM\alpha\mu b\sqrt{\rho_S} \tag{8}$$

Combining Eq. (3)–(5), we can get the measured nano-hardness:

$$H_{tested} = kM\alpha\mu b\sqrt{\rho_S + \rho_G} \tag{9}$$

Above consideration is the first step of the Nix-Gao model. However, the semi-spherical distribution assumption of GNDs in Nix-Gao model is not physically convincing, especially in the shallow area. Here, we show an analytical method to estimate the hardness without considering size effect, simply on the assumption that GND densities are the same (setting $\omega = 1$ in Eq. (12)) before and after irradiation, since ρ_G depends on the indentation depth only. The schematic of SSD and GND is shown in Fig. 3, indicating that SSD density is different before and after irradiation. Thus, at the same indention depth, the hardness follows the relations:

$$H_{tested,irr}^2 - H_{0,irr}^2 = (kM\alpha\mu b)^2\rho_{G,irr} \tag{10}$$

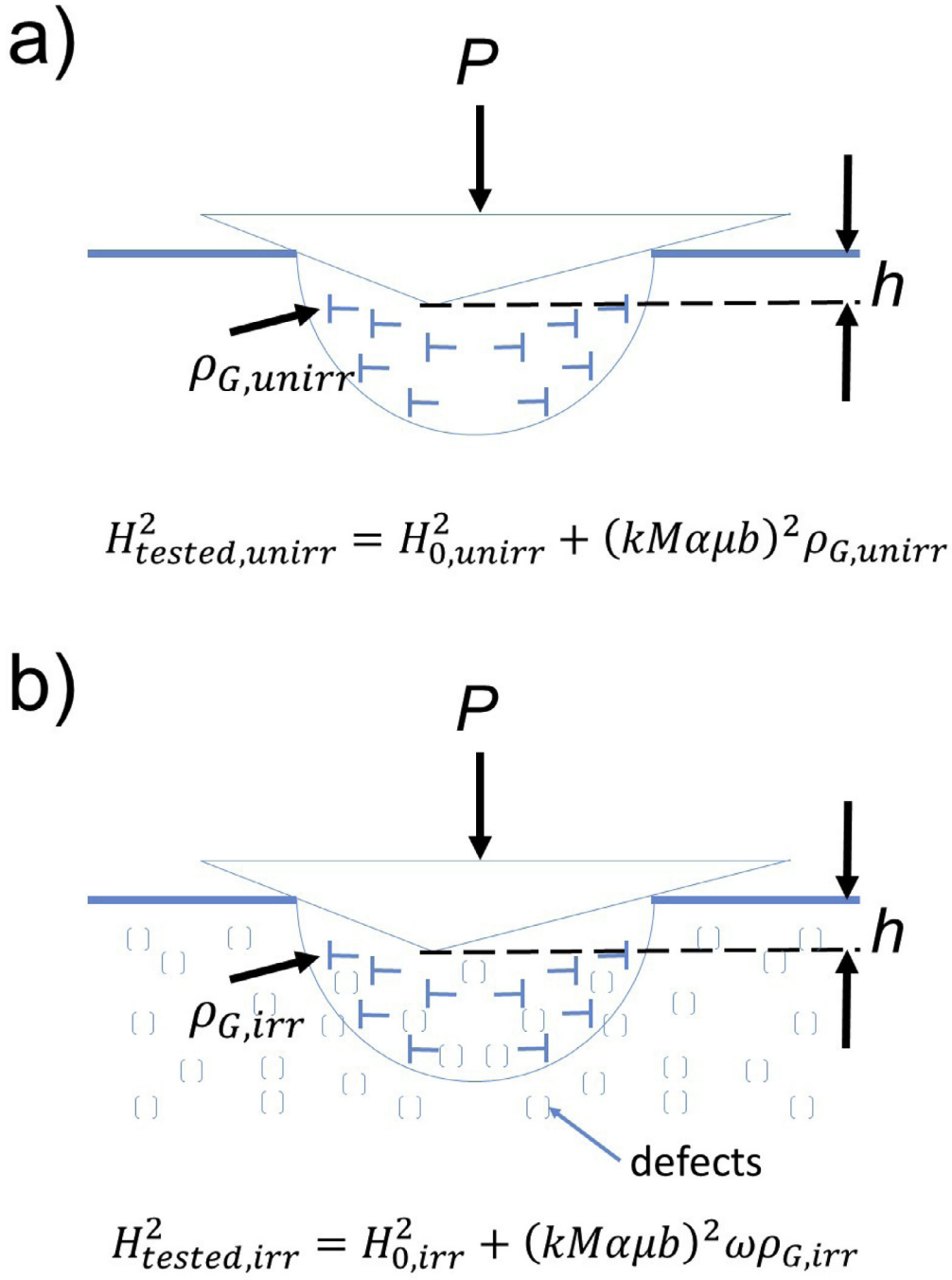

Fig. 3. Schematic diagrams of the distribution of SSD and GND in Nix-Gao model; (a) unirradiated, (b) irradiated.

$$H^2_{tested,unirr} - H^2_{0,unirr} = (kM\alpha\mu b)^2\rho_{G,unirr} \quad (11)$$

$$\rho_{G,irr} = \omega\rho_{G,unirr} \quad (12)$$

The subscript "irr" stands for irradiated sample, "unirr" stands for un-irradiated sample. Combining Eqs. (10)–(12) (setting $\omega = 1$), the following equation is finally obtained:

$$H_{0,irr} = \sqrt{H^2_{tested,irr} - H^2_{tested,unirr} + H^2_{0,unirr}} \quad (13)$$

$H_{tested,irr}$ and $H_{tested,unirr}$ are measured values obtained by nano-indentation tests. $H_{0,unirr}$ is the bulk-equivalent hardness of un-irradiated material, which could be estimated by the Nix-Gao model for deep depth [18].

Actually in the Nix-Gao model, the assumption that GNDs have the same distribution is pre-embedded in its semi-sphere refinement, whose radius equals to the radius of indenter contacted surface. Eq. (13) enables to give an application to calculate the hardness of the irradiated layer without discussing the real distribution or densities of GNDs.

4. Results and discussion

Figs. 4 and 5 show the depth dependence of the hardness before and after single-beam and dual-beam irradiation, respectively, for (a) as-received W and (b) recrystallized W. In the recrystallized W before irradiation, pop-in phenomena occurred even beyond 100 nm of indentation depth. Since the nano-hardness be-

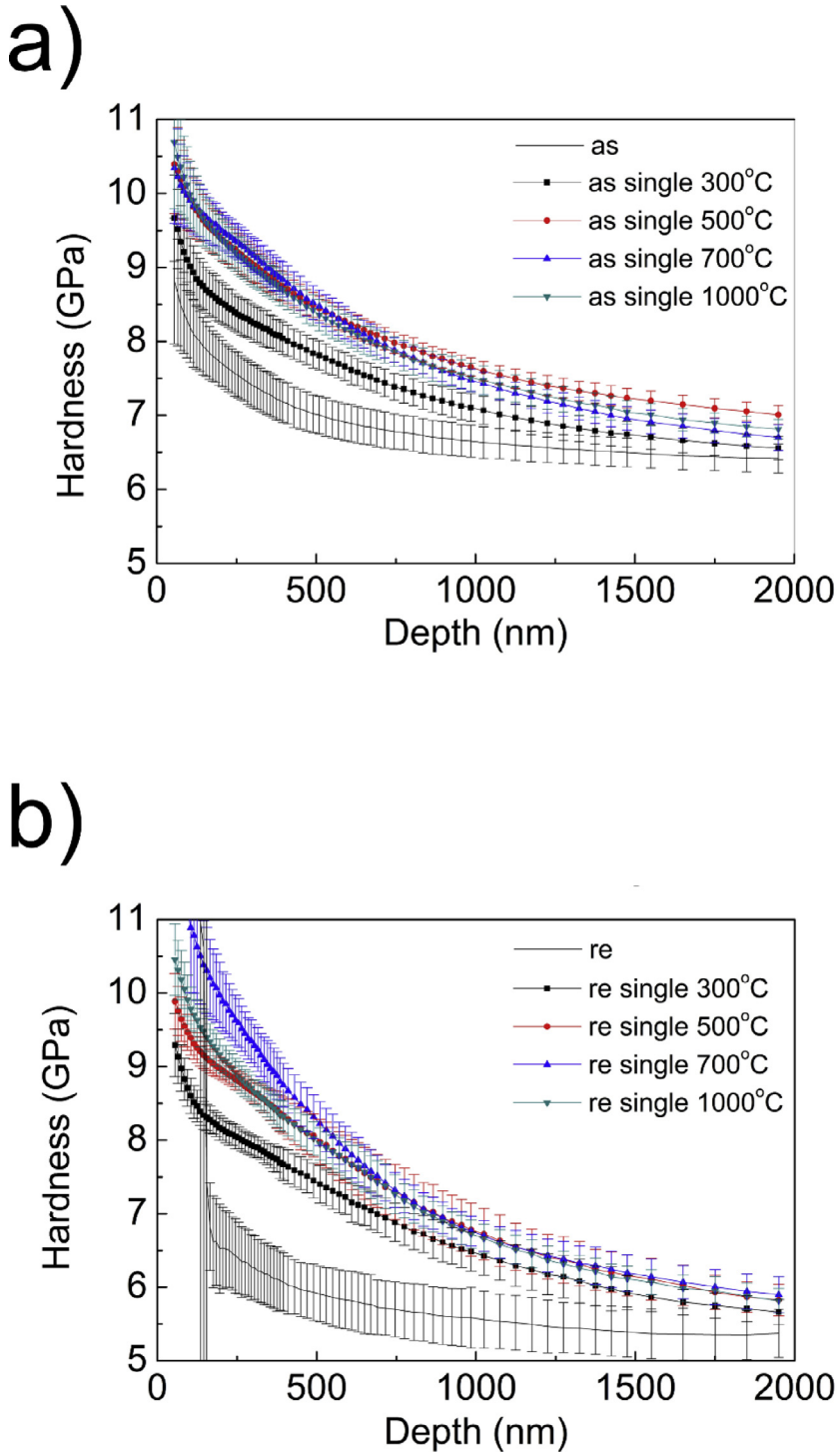

Fig. 4. The profiles of nano-indentation hardness in the direction of depth of (a) as-received and (b) recrystallized W before and after single beam irradiation.

low 100 nm was considered less reliable, the data obtained before the first pop-in were neglected. Size effect could be seen clearly in shallow area. The slopes became gentle over the indentation depth of 1000 nm. At all the tested conditions, the irradiation induced hardening in W. The hardness gradually decreased with increasing depth and became close to the unirradiated values, which can be explained that the plastic region by the indentation penetrates the damaged area and the contribution of the irradiation hardening becomes less at the deeper depth.

The bulk equivalent hardness, H_0, calculated by Eq. (13) is shown in Fig. 6 for single-beam irradiation and Fig. 7 for dual-beam irradiation. Figs. 6 (a) and 7 (a) are for as-received W, and Figs. 6 (b) and 7 (b) are for recrystallized W. The bulk equivalent hardness of the unirradiated samples was calculated by the Nix-Gao model with the plots in the depth from 1000 nm to 2000 nm. In the case of single-beam irradiation of as-received W (Fig. 6 (a)), the hardness is almost constant and appears to show a platform between 200 nm and 300 nm, indicating that the hardening of the

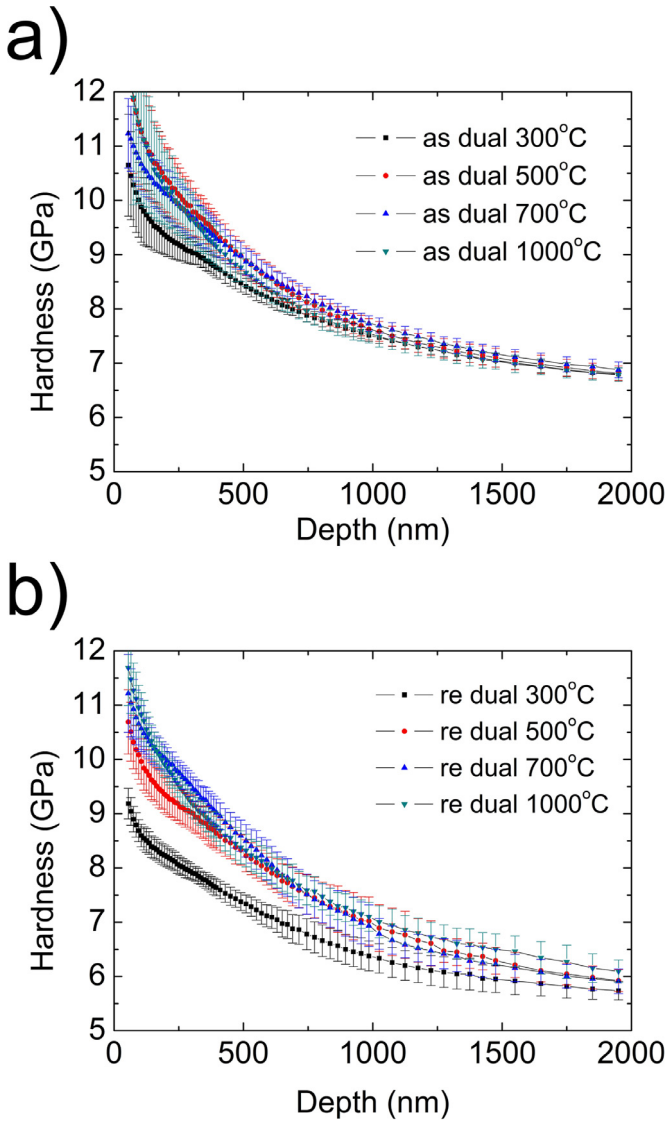

Fig. 5. The profiles of nano-indentation hardness in the direction of depth of (a) as-received and (b) recrystallized W after dual beam irradiation.

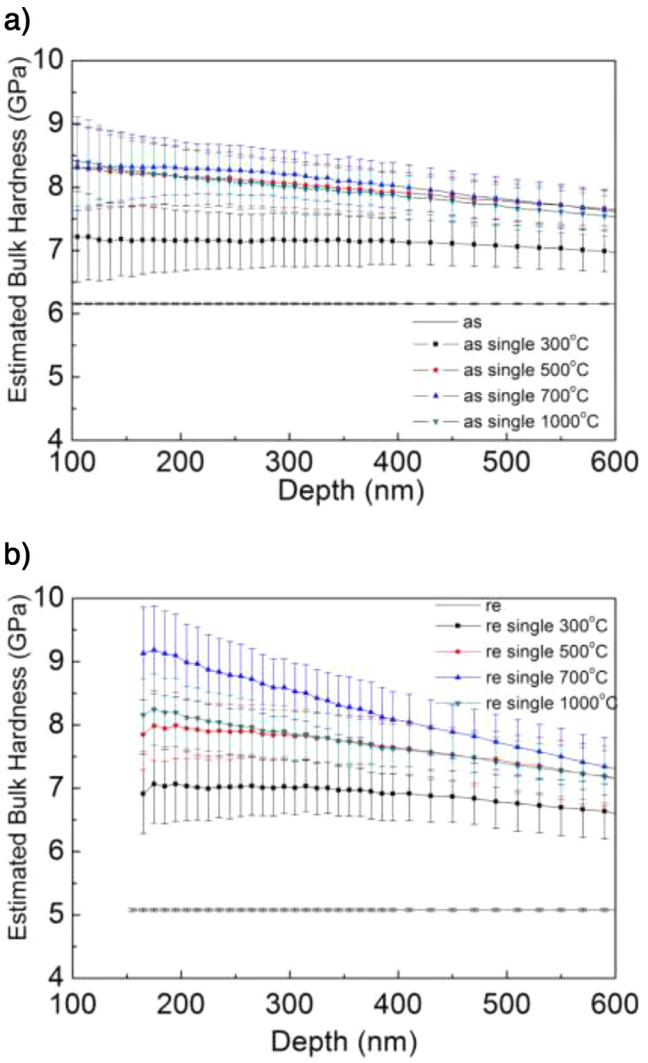

Fig. 6. The estimated bulk equivalent nano-hardness of W after single-beam irradiation at different temperatures; (a) as-received, (b) recrystallized.

plastically deformed area at different indentation depths is homogeneous.

Irradiation hardening was similar for the as-received W irradiated at 500 °C and 1000 °C, but the hardening appears to be higher at 700 °C in the case of single beam irradiation. At 300 °C, the hardening is less than those at higher temperatures. In the case of recrystallized W, the hardening showed higher hardening than at 300 °C, 500 °C and 1000 °C. The W irradiated at 500 °C and 1000 °C exhibited similar hardening effect, while the W irradiated at 300 °C showed the lowest hardening in the tested condition. In this tested temperature range, the trend of irradiation hardening agrees well with the one of neutron irradiated W [10].

TEM observations revealed that the typical distribution of microstructures in ion-irradiated W can be divided into two parts: the surface area with low density but larger size of defects, and the deeper area with small sizes of defects of high number density exhibiting a high contrast band after the peak position of dpa as shown in Fig. 1. Fig. 9 shows the cross sectional TEM micrographs of the damage distribution in the W irradiated with dual ion-beam at different temperatures. The distribution of the high contrast black bands clearly exceeded the damge peak position (about 1100 nm) and even the peak depth of implanted Fe ions (about 1300 nm) (Fig. 1). Ciupinski et al. [27] compared the microstructure distribution in W irradiated to different dpa level by self-ion implantation. The microstructure evolution is quite sensitive to dpa up to 0.1 dpa level. Grzonka et al. [28] suggested that the depth of the black band depends on the crystal orientation. In Fig. 8, with increasing temperature, diffusion of microstructures becomes significant, for example, in the case of the dual-beam irradiation at 1000 °C, the diffused interstitial atoms were formed into small dot-like structures at a depth of 4 μm.

Comparing the defect distribution and the hardening behavior shown in Figs. 4–7, the position of the black band seems to give little effect on the irradiation hardening, since the hardness profile curves didn't show significant change in the deeper and stable area. Therefore, the hardness in the stable area could reflect the hardness involving the whole irradiation area. Here the average value between the depth of 240–250 nm, which was in the platform of the calculated hardness values, was chosen as the reference depth to define the hardness before and after irradiation, and the hardening calculated by $\Delta H = H_{0,irr} - H_{0,unirr}$ is shown in Fig. 9.

As shown in Fig. 9, the ion-irradiation of W resulted in hardening at all the irradiation temperatures up to 1000 °C. The effect of helium in as-received W is much larger than that in recrystallized W: dual-beam irradiation enhanced the irradiation hardening com-

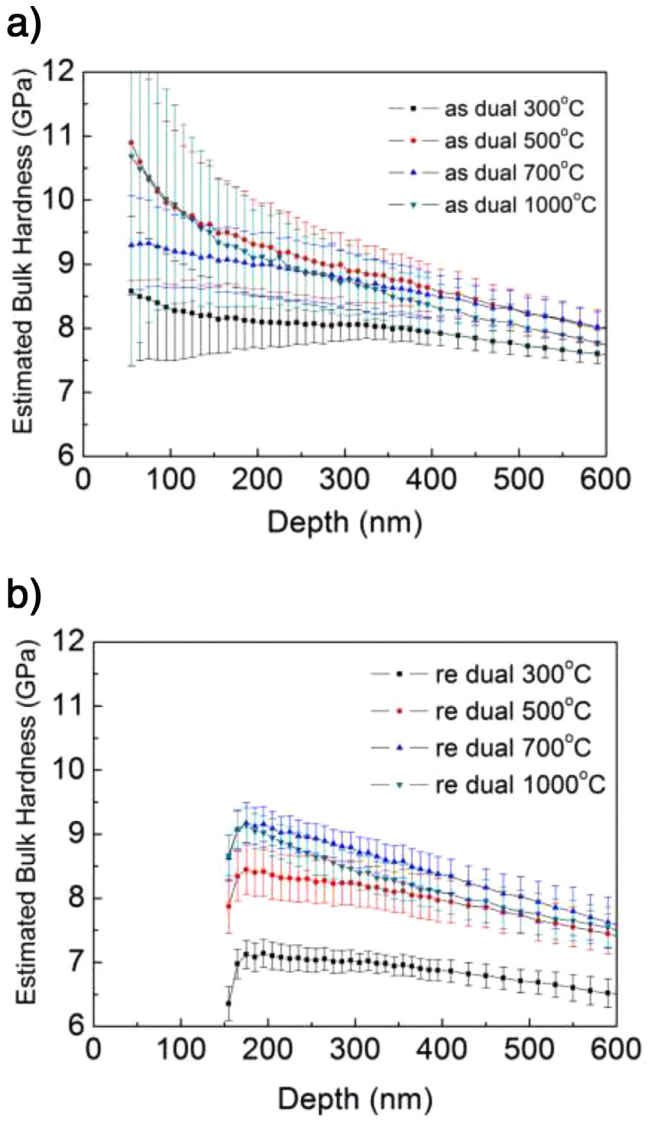

Fig. 7. The estimated bulk equivalent nano-hardness of W after dual beam irradiation at different temperatures (a) as-received, (b) recrystallized.

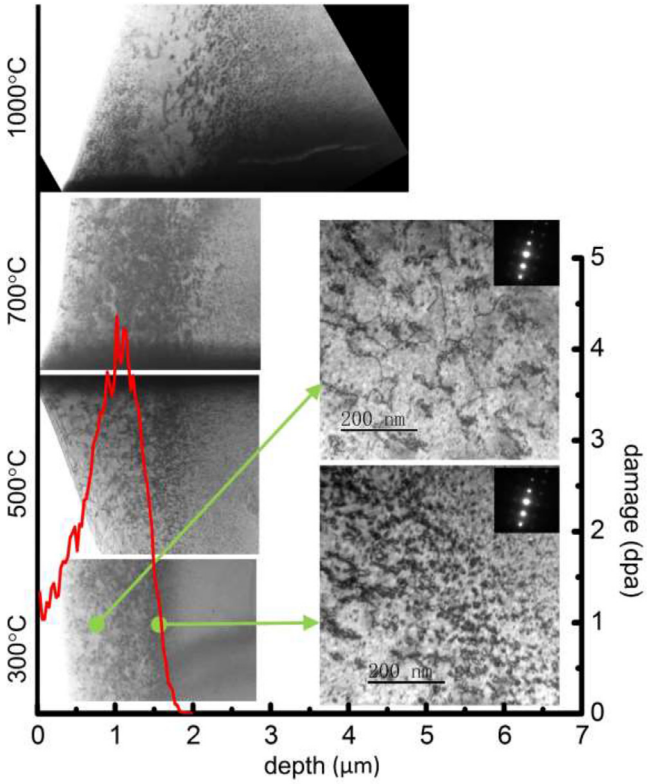

Fig. 8. TEM images of recrystallized W after dual beam irradiation at different temperatures.

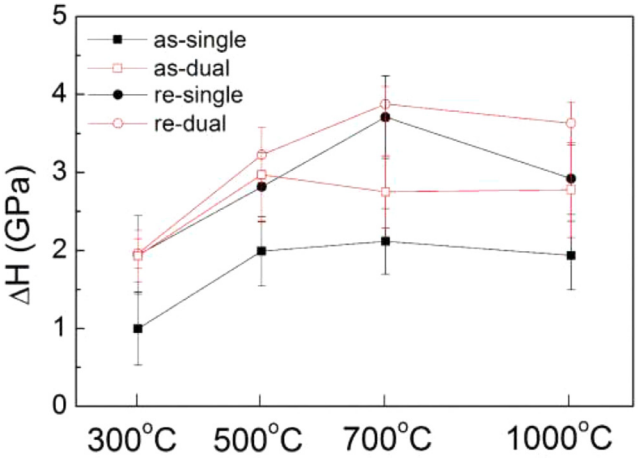

Fig. 9. The irradiation hardening of W after single- and dual-beam irradiation at different temperatures.

pared with single-beam in as-received W. The smallest irradiation hardening was observed at 300 °C for both single and dual-beam irradiation, but the irradiation hardening was almost independent of the irradiation temperature from 500 °C to 1000 °C. For the recrystallized W, the irradiation hardening increased at the irradiation temperature from 300 °C to 700 °C, but decreased from 700 °C to 1000 °C. No significant effect of helium was observed at the irradiation temperature from 300 °C to 700 °C. However, at the irradiation temperature of 1000 °C, dual-beam irradiation caused larger irradiation hardening than single-beam irradiation.

The recrystallized W showed a larger irradiation hardening than as-received W. The reason could be owing to the grain-boundary effect. The grain-boundaries can act as sinks for interstitials and vacancies, the defects will grow less in as-received W, because the grain boundary area in recrystallized W is smaller than that in as-received one. In the case of irradiation at 1000 °C, the distribution of loops extended only to 1.3 μm depth but voids were found even at 2 μm. The defects showed stratification in the irradiated area, which is quite different from the lower temperature irradiations. How the microstructures correlated with the hardness will be investigated in the future work by an Orowan type equation, where the size and number density of dislocations and cavities will be analyzed by TEM. The main issues of nano-indentation application to ion-irradiation hardening in future will be addressed on (1) How to precisely evaluate the bulk-equivalent hardness through nano-indentation and (2) How to deal with the hardening contribution of the inhomogeneously distributed defects in the irradiated layer. The method and results described in this paper may offer a way to help solve these problems.

5. Summary and conclusion

As-received and recrystallized W were irradiated with single-beam of 6.4 MeV Fe^{3+} or dual-beam of 6.4 MeV Fe^{3+} + 1 MeV(energy degraded) He^{+} at 300 °C, 500 °C, 700 °C and 1000 °C.

Irradiation hardening was measured by the nano-indentation method.

(1) An equation to evaluate the irradiation hardening was shown based on the assumption that GND densities at an indentation depth were the same before and after irradiation.
(2) The obtained depth profile of the bulk equivalent hardness showed almost constant values in the range from 200 nm to 300 nm, indicating that the estimated irradiation hardening derived by this method (Eq. (13)) is unaffected by the indentation size effect.
(3) Ion-irradiation always induces hardening in both as-received and recrystallized W at all the irradiation temperatures. In the case of single-beam irradiation, recrystallized W exhibited higher hardening than as-received one, which can be interpreted in terms of defect sink at grain boundaries in as-received W.
(4) The effect of helium on the irradiation hardening is dependent on the material condition: as-received W showed an additional hardening by helium at all the irradiation temperatures, while in recrystallized W the hardening was not affected by helium at 700°C and below.

Acknowledgments

We thank Dr. Kasada for his cooperation measuring nano-indentation hardness. Mr. Hashitomi and Dr. Kondo are acknowledged for operating DuET, Kyoto University. China Scholarship Council was thanked for sponsoring the corresponding author with overseas study expense.

References

[1] X. Yi, M.L. Jenkins, M. Briceno, S.G. Roberts, Z. Zhou, M.A. Kirk, In situ study of self-ion irradiation damage in W and W-5Re at 500 °C, Philos. Mag. 93 (2013) 1715–1738.
[2] O. El-Atwani, A. Suslova, T.J. Novakowski, K. Hattar, M. Efe, S.S. Harilal, A. Hassanein, In-situ TEM/heavy ion irradiation on ultrafine-and nanocrystalline–grained tungsten: effect of 3 MeV Si, Cu and W ions, Mater. Characterization 99 (2015) 68–76.
[3] X.O. Yi, M.L. Jenkins, K. Hattar, P.D. Edmondson, S.G. Roberts, Characterisation of radiation damage in W and W-based alloys from 2 MeV self-ion near-bulk implantations, Acta Materialia 92 (2015) 163–177.
[4] Y. Himei, K. Yabuuchi, R. Kasada, S. Noh, H. Noto, T. Nagasaka, S. Nogami, A. Kimura, Ion-Irradiation Hardening of Brazed Joints of Tungsten and Oxide Dispersion Strengthened (ODS) Ferritic Steel, Mater. Trans. 54 (2013) 446–450.
[5] H.W. Wang, Y. Gao, E.G. Fu, T.F. Yang, S. Yan, J.M. Xue, P.K. Chu, Y.G. Wang, Effect of high fluence Au ion irradiation on nanocrystalline tungsten film, J. Nucl. Mater. 442 (2013) 189–194.
[6] S. Kajita, N. Yoshida, N. Ohno, Y. Hirahata, R. Yoshihara, Helium plasma irradiation on single crystal tungsten and undersized atom doped tungsten alloys, Physica Scripta 89 (2014) 7.
[7] S. Kajita, N. Yoshida, N. Ohno, Y. Tsuji, Growth of multifractal tungsten nanostructure by He bubble induced directional swelling, New J. Phys. 17 (2015) 14.
[8] M.H. Cui, Z.G. Wang, L.L. Pang, T.L. Shen, C.F. Yao, B.S. Li, J.Y. Li, X.Z. Cao, P. Zhang, J.R. Sun, Y.B. Zhu, Y.F. Li, Y.B. Sheng, Temperature dependent defects evolution and hardening of tungsten induced by 200 keV He-ions, Nucl. Instrum. Methods Phys. Res. Sect. B-Beam Interact. Mater. Atoms 307 (2013) 507–511.
[9] H. Watanabe, N. Futagami, S. Naitou, N. Yoshida, Microstructure and thermal desorption of deuterium in heavy-ion-irradiated pure tungsten, J. Nucl. Mater. 455 (2014) 51–55.
[10] M. Fukuda, A. Hasegawa, S. Nogami, K. Yabuuchi, Microstructure development of dispersion-strengthened tungsten due to neutron irradiation, J. Nucl. Mater. 449 (2014) 213–218.
[11] M. Fukuda, A. Hasegawa, T. Tanno, S. Nogami, H. Kurishita, Property change of advanced tungsten alloys due to neutron irradiation, J. Nucl. Mater. 442 (2013) S273–S276.
[12] D.E.J. Armstrong, P.D. Edmondson, S.G. Roberts, Effects of sequential tungsten and helium ion implantation on nano-indentation hardness of tungsten, Appl. Phys. Lett. 102 (2013) 5.
[13] D.E.J. Armstrong, X. Yi, E.A. Marquis, S.G. Roberts, Hardening of self ion implanted tungsten and tungsten 5-wt% rhenium, J. Nucl. Mater. 432 (2013) 428–436.
[14] J. Gibson, S.G. Roberts, D.E.J. Armstrong, High temperature indentation of helium-implanted tungsten, Mater. Sci. Eng.-Struct. Mater. Properties Microstruct. Process. 625 (2015) 380–384.
[15] W.D. Nix, H.J. Gao, Indentation size effects in crystalline materials: A law for strain gradient plasticity, J. Mech. Phys. Solid 46 (1998) 411–425.
[16] R. Kasada, Y. Takayama, K. Yabuuchi, A. Kimura, A new approach to evaluate irradiation hardening of ion-irradiated ferritic alloys by nano-indentation techniques, Fusion Eng. Des. 86 (2011) 2658–2661.
[17] R. Kasada, S. Konishi, K. Yabuuchi, S. Nogami, M. Ando, D. Hamaguchi, H. Tanigawa, Depth-dependent nanoindentation hardness of reduced-activation ferritic steels after MeV Fe-ion irradiation, Fusion Eng. Des. 89 (2014) 1637–1641.
[18] G.M. Pharr, E.G. Herbert, Y.F. Gao, The Indentation Size Effect: A Critical Examination of Experimental Observations and Mechanistic Interpretations, Annu. Rev. Mater. Res. 40 (2010) 271–292.
[19] Y. Huang, F. Zhang, K.C. Hwang, W.D. Nix, G.M. Pharr, G. Feng, A model of size effects in nano-indentation, J. Mech. Phys. Solid 54 (2006) 1668–1686.
[20] D. Kiener, R. Pippan, C. Motz, H. Kreuzer, Microstructural evolution of the deformed volume beneath microindents in tungsten and copper, Acta Materialia 54 (2006) 2801–2811.
[21] Y. Katoh, M. Ando, A. Kohyama, Radiation and helium effects on microstructures, nano-indentation properties and deformation behavior in ferrous alloys, J. Nucl. Mater. 323 (2003) 251–262.
[22] http://www.srim.org/.
[23] R.E. Stoller, M.B. Toloczko, G.S. Was, A.G. Certain, S. Dwaraknath, F.A. Garner, On the use of SRIM for computing radiation damage exposure, Nucl. Instrum. Methods Phys. Res. Sect. B-Beam Interact. Mater. Atoms 310 (2013) 75–80.
[24] ASTM, Standard Practice for Neutron Radiation Damage Simulation by Charged-Particle Irradaition, in: E521-96, 2009.
[25] W.C. Oliver, G.M. Pharr, An improved technique for determining hardness and elastic-modulus using load and displacement sensing indentation experiments, J. Mater. Res. 7 (1992) 1564–1583.
[26] G.Z. Voyiadjis, R. Peters, Size effects in nanoindentation: an experimental and analytical study, Acta Mechanica 211 (2010) 131–153.
[27] L. Ciupinski, O.V. Ogorodnikova, T. Plocinski, M. Andrzejczuk, M. Rasinski, M. Mayer, K.J. Kurzydlowski, TEM observations of radiation damage in tungsten irradiated by 20 MeV W ions, Nucl. Instrum. Methods Phys. Res. Sect. B-Beam Interact. Mater. Atoms 317 (2013) 159–164.
[28] J. Grzonka, L. Ciupinski, J. Smalc-Koziorowska, O.V. Ogorodnikova, M. Mayer, K.J. Kurzydlowski, Electron microscopy observations of radiation damage in irradiated and annealed tungsten, Nucl. Instrum. Methods Phys. Res. Sect. B-Beam Interact. Mater. Atoms 340 (2014) 27–33.